A simplified first-principles model of a compact flotation unit for use in optimization and control

Tamal Das and Johannes Jäschke*

Department of Chemical Engineering, Norwegian University of Science and Technology
Sem Sælandsvei 4, 7491 Trondheim, Norway

E-mail: jaschke@ntnu.no

Abstract

In this paper, we develop a simplified control-oriented model of a compact flotation unit (CFU), which removes residual oil from produced water in oil and gas production systems. CFU is a class of separators that exploits the synergy between separation effects of a swirling flow and the effect of flotation, in which small gas bubbles attach to the oil droplets, and float to the top of the separator, where they are removed. The purified water flows downwards, and is removed from the bottom. Our CFU model consists of a simplified initial swirl separation part, and a flotation part, in which populations of oil droplets, gas bubbles without oil droplet, and gas bubbles with oil droplet attached are tracked spatially. After analyzing the model, we use it as a basis for designing a control structure that operates the separation system optimally.

Introduction

In oil and gas production, besides hydrocarbons a significant amount of water is produced from the reservoirs. Such water is called produced water, and it must be cleaned from hydrocarbons before it can be discharged into the environment or re-injected into a reservoir. For

an overview of the different technologies available for produced water treatment within oil and gas industry, we refer to Fakhru'l-Razi et al..[1] The amount of dispersed oil in produced water that can be discharged to the sea is maximally 30 mg/l (≈ 30 *ppm*) as per OSPAR Recommendation 2001/1 (OSPAR is the convention for the Protection of the Marine Environment of the North-East Atlantic).[2] Also for water re-injection into the reservoir, it is important that the water has very low oil content, as well as is low on other metrics, such as turbidity or volatile suspended solids (VSS), otherwise there is a risk of clogging of the pores of the reservoir.[3]

Traditionally, the separation of oil and water has been performed in topside facilities or onshore in large vessels, but in recent years there has been an interest in developing compact separation systems that can be placed on the seabed or on small unmanned platforms. The oil industry has, therefore, been especially interested in compact technologies not only for bulk separation but also for high purity separation, such as hydrocyclones and compact flotation units (CFU), in order to obtain the desired oil content in water. The term compact flotation unit does not denote a single technology, but rather a range of technologies that combine the separation effect of swirling flows with a flotation mechanism. Many different designs have been developed by industrial vendors, of which the more complex designs involve a combination of induced and dissolved gas flotation, as well as several swirl and flotation stages.

Due to a low residence time in compact separation equipment and due to several degrees of freedom in operation, these compact systems, in comparison to conventional separation technologies, are more difficult to operate, and require more advanced control strategies.[4,5] Control of CFUs has been studied experimentally by Asdahl and Rabe,[5] and Arvoh et al.,[4,6] who analyze the effect of changing the reject valve position and CFU pressure on gas and liquid reject flow rates. These relationships helped them to develop a control system for CFU that optimizes separation efficiency and reject flow rate, and minimizes flotation gas usage using an automatic empirical approach.[5] However, to the authors' knowledge, there

has been no analysis of CFU operation based on models - a gap we fill in this paper.

The first contribution of this paper is a control-oriented model of a CFU that is based on physical insight, and that is suitable for use in modern control, optimization and estimation algorithms. This model can be used to describe the effect of important disturbances, such as inlet water flow rate, and inlet oil concentration on processed water quality. Besides, it also captures the response of oil content in water outlet and the separation efficiency to changes in flotation gas rate. The second contribution of this paper is the development of a control structure based on this model, together with a thorough study of the performance of this control structure under various disturbances.

CFU technology

Concept of flotation

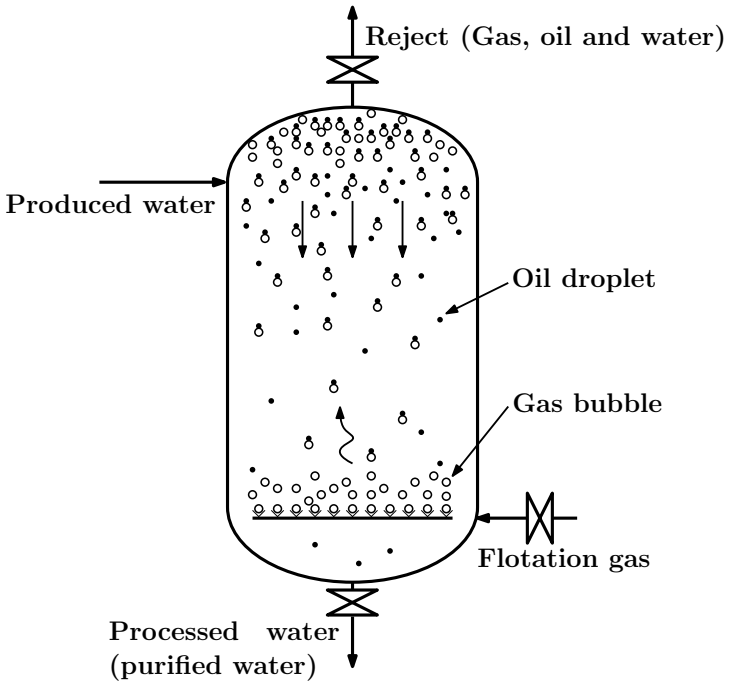

Figure 1: Schematic of a flotation device. The figure shows how gas bubbles of the flotation gas attach to oil droplets as they rise upwards. The gas bubbles, either loaded with oil or free, get accumulated at the top and are removed via the reject stream. The purified water is removed at the bottom.

A flotation device is shown schematically in Figure 1. The main concept of flotation is that the produced water containing small droplets of oil is fed into a vessel, and flows downwards towards the bottom of the device. Flotation gas is injected into the separator and forms tiny bubbles. These bubbles travel upwards, and along the way attach to oil droplets and drag them to the top, where the oil and gas is removed in the reject stream. The reject typically also contains some water while rest of the water gets cleaner and cleaner as it travels downwards. Finally, the purified water is removed from the bottom.

Mechanisms affecting the flotation process in produced water treatment have been described e.g. by Frankiewicz et al.[7] According to them, a low contact angle between the oil droplet and the gas bubble facilitates either oil coating the gas bubbles or oil sticking to the gas bubbles, both of which lead to oil floating to the top with the gas bubbles. A third scenario in which oil forms a lens near the inner bottom edge of the bubble is also possible.[8] The three scenarios are shown in Figure 2.

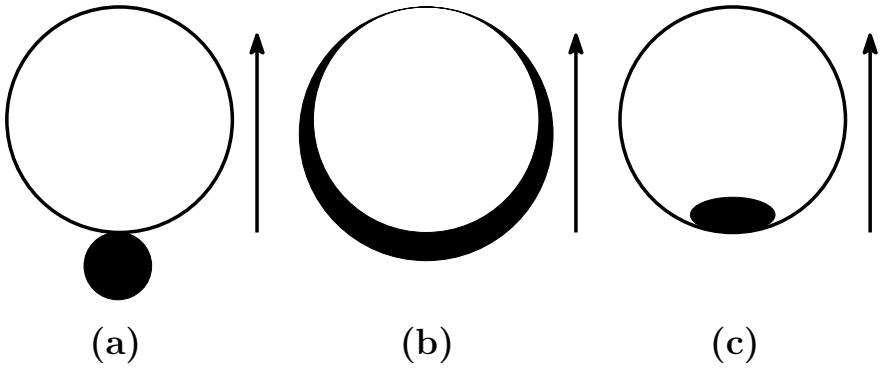

Figure 2: Scenarios after collision between droplets and bubbles: (a) Point attachment, (b) Oil film and (c) Oil lens (adapted from Rawlins and Ly[8]).

For effective separation, the conditions in the separator must enable a good contact between the gas bubbles and the oil droplets. This means that the number density of the droplets and the bubbles should be sufficiently large to ensure a high collision frequency between these two populations. From this perspective, many small bubbles are better than few large bubbles, as a high number density results in a higher probability of collision.[7]

Gas flotation can be realized by two different techniques - induced gas flotation (IGF)

and dissolved gas flotation (DGF). In induced gas flotation, illustrated in Figure 3 top, the injected gas directly forms bubbles of diameters in the range of 100-1000 μm. As IGF results in relatively large bubbles, the bubbles have a high rising velocity, which makes it suitable to inject the gas at the bottom of the separator. In dissolved gas flotation, as shown in Figure 3 bottom, the gas enters the separator saturated in a liquid at high pressure. When the pressure is reduced, bubbles of gas form. This technique yields smaller bubbles in the range of $10 - 100$ μm in diameter.[9] Modern CFU designs combine the two flotation methods as there are disadvantages of using only one. In DGF systems, oil droplets larger than 100 μm cannot be floated, because the volume of the gas bubbles is not high enough to ensure that they attach to the oil droplets and successfully rise to the top of the separator. On the other hand, in IGF systems, oil droplets with sizes much smaller than 100 μm may escape flotation, as small oil droplets do not attach well to large gas bubbles.

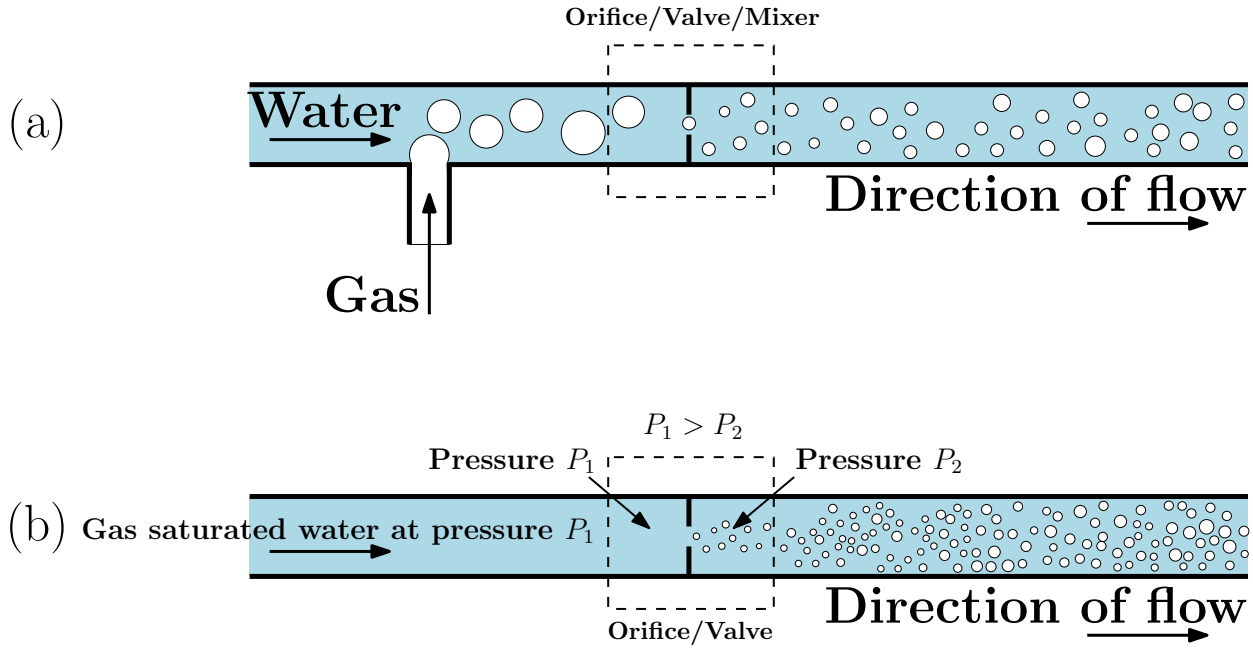

Figure 3: Gas flotation methods: (a) Induced gas flotation and (b) Dissolved gas flotation (adapted from Shannon[10]).

A compact flotation unit design with induced gas flotation

As mentioned above, there are several CFU designs, many of which have resulted due to a continuous improvement over previous designs.[11–13] In this paper we consider a simple CFU design that uses IGF with flotation gas fed at the bottom, as shown in Figure 4. A similar design has been proposed by e.g. the *NATCO Group Inc.*[7] A feed of oily water enters at the top of the separator and undergoes a swirling motion at the start, which causes some of the oil droplets to separate at the top, while the rest of the oily water flows downwards. A swarm of gas bubbles is injected continuously at the bottom of the separator. These bubbles stick to or get coated with the oil droplets in the water, and carry them to the top. The flotation gas flow is typically 10% (volume/volume) of the incoming water flow.[14] At the top of the CFU, the collected oil and gas along with some water is removed through the reject stream. The liquid flow in the reject stream at the top is typically maintained at around 1% of the incoming water flow[5] and the purified water typically has an oil concentration below 30 *ppm*.

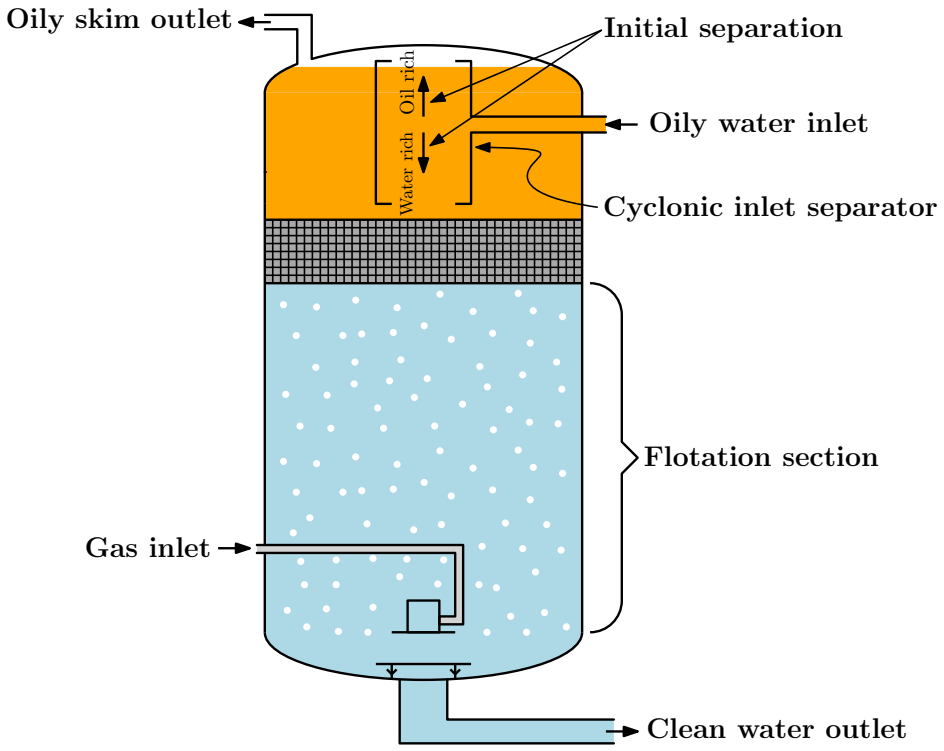

Figure 4: Simple CFU design considered in this paper.

Control-oriented CFU model

Modeling concept and assumptions

The schematic of our CFU model is given in Figure 5. The feed enters first into the swirl part, where an initial separation of part of the oil takes place. Then, the water with the remaining oil enters the flotation section. The model of the flotation section is based on mass

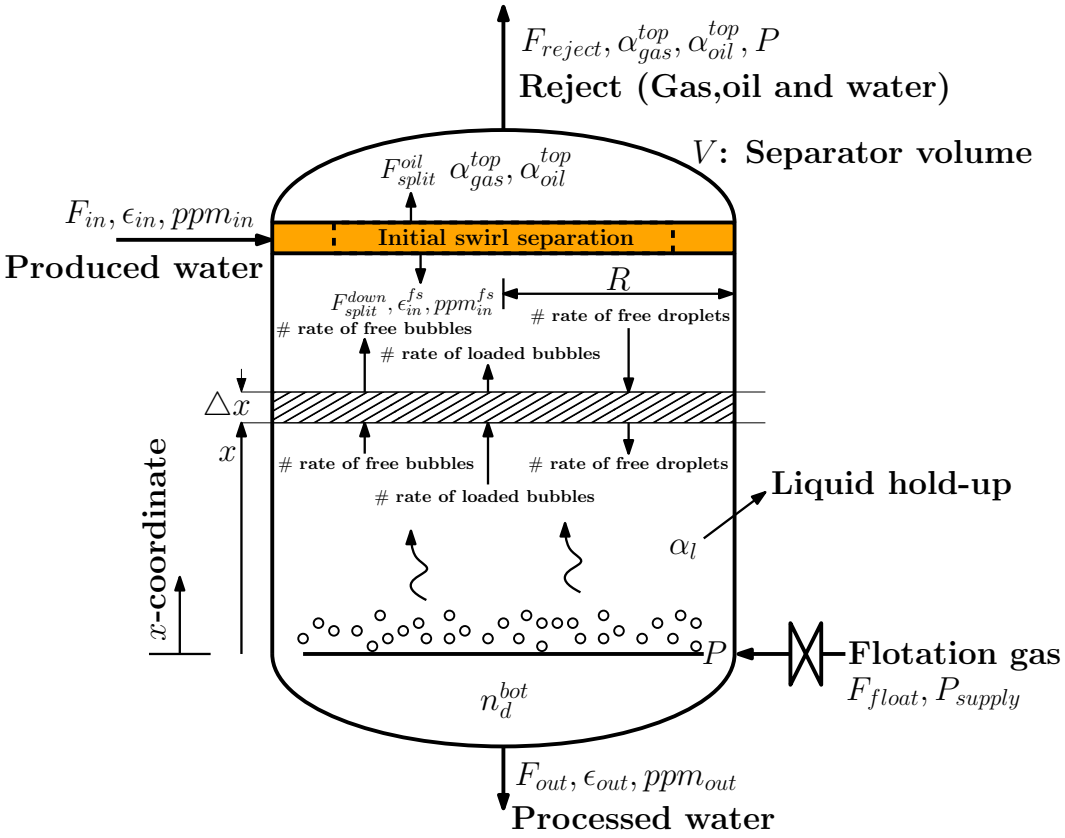

Figure 5: Schematic view of the CFU model. All the important variables used in the model are indicated.

balances for three entities: free gas bubbles, free oil droplets and loaded bubbles. A loaded bubble results from a merger of one oil droplet and one gas bubble as shown in Figure 6. The free gas bubbles and the loaded bubbles move upwards, whereas the oil droplets move downwards. The free bubbles and the loaded bubbles leave the CFU through the reject stream at the top. Other major assumptions made are as follows:

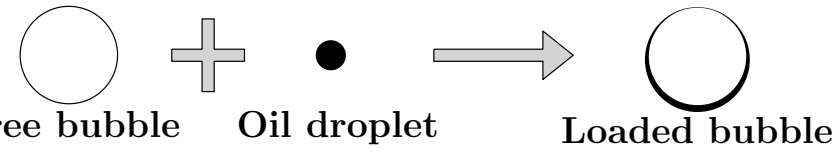

Figure 6: Representation of loading process as a combination of an oil droplet and a free bubble.

1. All liquid is assumed incompressible.

2. Gas is modeled by ideal gas law.

3. The swirl effect is dependent on the inflow and is captured in the initial swirl separation part. In the flotation model, the swirl effect is assumed to be negligible[1].

4. After the initial swirl separation, the water continuum (bulk phase) is uniformly distributed and moves down at a constant velocity as a plug flow.

5. All oil droplets are assumed spherical, have the same representative diameter, and are uniformly distributed in the horizontal cross section of the vessel. As oil droplets go through swirling effect in initial separation of CFU as shown in Figure 5, they coalesce and then represent a sharp distribution with majority of droplets having similar size.

6. The oil droplets have a terminal velocity relative to the continuous water phase given by the Stokes' law.

7. The loaded bubbles and the free bubbles assume terminal velocities given by Stokes' law.

8. All bubbles - loaded and free - are of spherical shape.

9. All gas bubbles are assumed to have the same diameter and each gas bubble can float at most one oil droplet.

[1]As we will see later, this assumption can be relaxed somewhat by adapting the collision efficiency in the flotation part.

10. The size of the bubbles (free as well as loaded) is assumed to be not affected by the pressure gradient along the height of the separator because the pressure difference between top and bottom of the separator does not affect the bubble sizes significantly.

11. The volume of a loaded bubble is the sum of the droplet volume and the bubble volume.

12. Free and loaded bubbles rise while oil droplets move downwards with the bulk.

13. The device used to produce gas bubbles in the CFU is designed to deliver bubbles of a fixed standard size.

14. The amount of oil and gas dissolved in the water is negligible.

Simplified initial swirl separation model

The initial separation due to swirling effect causes oil droplets to travel towards the center radially due to cyclonic forces, which leads to small droplets coalescing to become larger droplets. Also, the turbulent flow enables a higher collision frequency between the droplets, and therefore, facilitates coalescence. The larger droplets have a higher rise velocity, such that they move upwards to enter the top part of the swirl separator and get separated. We assume that this phenomenon happens relatively fast. Hence, we model it as a static split called swirl split. In particular, the swirl split of the initial separator is defined as $\epsilon_{in}^{fs}/\epsilon_{in}$, that is the ratio of the oil cut ϵ_{in}^{fs} of water entering the flotation section, to the feed concentration ϵ_{in}. We propose to model the effect of the swirl separator as a function of swirl intensity S, which is a measure of the strength of the swirl effect, such that

$$\frac{\epsilon_{in}^{fs}}{\epsilon_{in}} = A(S-B)^2 + C, \tag{1}$$

where, the parameters are swirl split pre-factor A, optimum swirl intensity B and optimum swirl split C. The swirl intensity S is assumed to be linearly dependent on inflow F_{in} as

$$S = DF_{in}, \tag{2}$$

where, D denotes swirl intensity pre-factor. This assumption is an extension of the linear dependence of the maximum tangential velocity to inflow that is used in equation (3.5) in work of Tyvold.[15]

The swirl split from Eq. 1 is shown for a chosen set of parameters in Figure 7. It reflects the fact that the swirling effect improves separation only up to a certain optimal swirl intensity, which is assumed to be of value B here. Beyond the optimal swirl intensity, breakage of droplets due to the momentum of the swirl dominates over the coalescence effects, and the separation efficiency of the initial swirl separation deteriorates. In the proposed

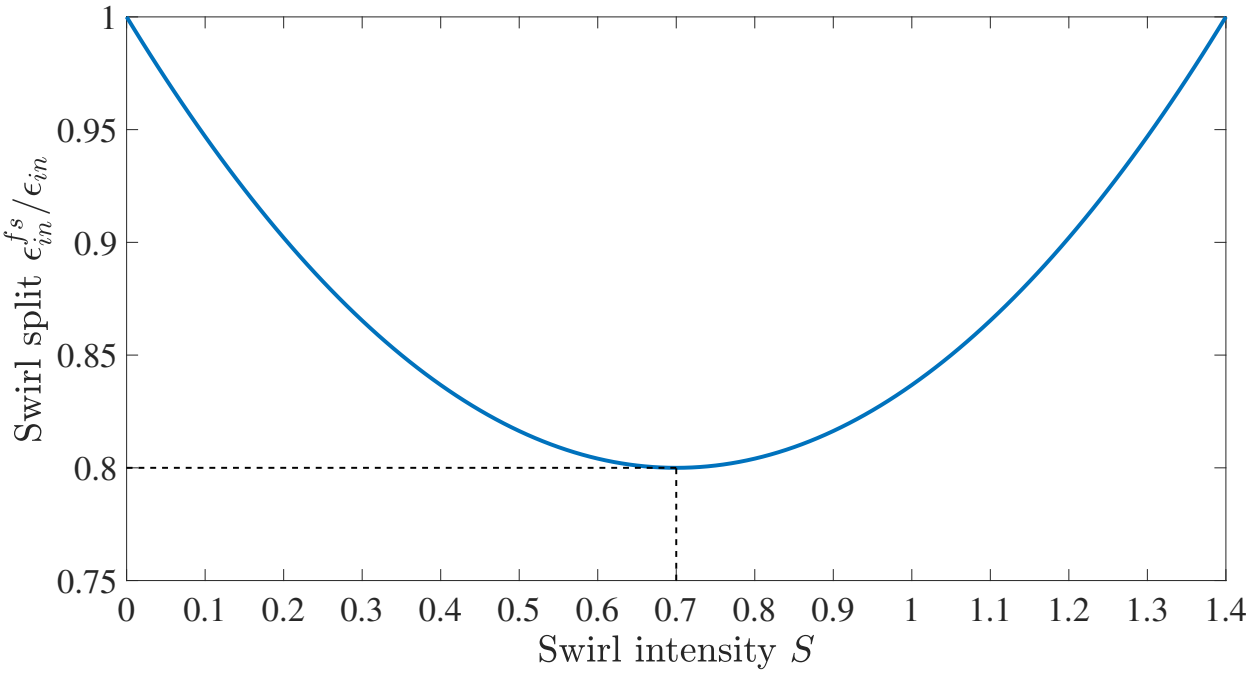

Figure 7: Swirl split as a function of swirl intensity S presented with optimum swirl intensity $B = 0.7$, optimum swirl split $C = 0.8$. Pre-factor A is chosen 0.4082 such that for zero inflow, which also means zero swirl intensity, i.e. $S = 0$, swirl split is 1, indicating no initial separation.

relationship in Eq. 1 the swirl split assumes the lowest value of C at an optimum swirl intensity B. For all other values of swirl intensity, $\epsilon_{in}^{fs}/\epsilon_{in}$ will be higher than B, indicating poorer initial separation.

Flotation model

Bubble loading model

The separation dynamics in the flotation model are governed by a specific bubble loading rate, which is related to the rate of "successful" collisions between bubbles and oil droplets. A successful collision is defined as one in which attachment between the droplet and the bubble happens. The collision efficiency E_c is defined analogous to that in a reaction rate for a reactive system as[16]

$$L_R = E_c n_{fb} n_d, \tag{3}$$

where, L_R is the loading rate, and n_{fb} and n_d represent the local number density (volumetric) of free bubbles and droplets, respectively. The collision efficiency E_c is a function of droplet and bubble sizes as given by[16]

$$E_c = k \left(\frac{d_d}{d_b} \right)^2, \tag{4}$$

where, d_b and d_d are bubble and droplet diameters, respectively, and k is a tuning parameter that governs the kinetics of the loading phenomenon.

Remark. *We have assumed perfect plug flow and no swirl in the flotation section. If, however, the swirl effect, or other turbulent and non-ideal effects need to be considered in the flotation section, they can be absorbed into the parameter k. For example, one may use operational data to fit a function $k = f(F_{in})$, and then use this instead of a constant value.*

Mass Balances

The feed F_{in} containing oil and water is fed into the initial swirl separation and splits into two flows - the separated oil flow F_{split}^{oil} that enters the top section, and the rest flow F_{split}^{down}

with oil concentration ϵ_{in}^{fs} that enters the flotation section from the top, while the flotation gas is injected between the flotation section and the bottom section, see Figure 8.

In our model we use the following notation (see also Figure 5): F_{in} for the oily water inflow rate, ϵ_{in} for inlet oil in water content (volume/volume) in water feed, which in *ppm* terms is denoted as ppm_{in}, F_{split}^{oil} for oil flow that is separated due to initial separation and travels upwards, F_{split}^{down} for the part of inflow F_{in} that travels downwards containing an oil concentration of ϵ_{in}^{fs}, which in *ppm* terms is denoted as ppm_{in}^{fs}, F_{out} for water outflow rate, ϵ_{out} for outlet oil in water content (volume/volume) in water outflow, which in *ppm* terms is denoted as ppm_{out}, F_{float} for flotation gas rate, F_{reject} for the total multiphase reject flow rate and α_{gas}^{top} and α_{oil}^{top} for volume fractions of gas and oil, respectively in the reject stream as well as in the top section. The model implements a mass balance on each of the entities - free bubbles, loaded bubbles and oil droplets - over several control volumes. Since the bubbles and droplets are assumed to be of a single representative size each throughout the separator, writing a balance on the number of these entities is equivalent to writing mass balances. The control volumes are segments of the CFU, with each control volume of the shape of a flat cylinder as shown in Figure 8. Hence, we present a number balance for each entity in one control volume of length $\triangle L$ and cross section area πR^2, with $\triangle V$ as the section volume,

$$\triangle V = \pi R^2 \triangle L. \tag{5}$$

We divide the flotation section of the CFU into 3 sections (see Figure 8) - a top section, from which oil, gas and some water is removed, a flotation section, where the flotation is taking place, and a bottom section, where the purified water is removed. We consider a total of $(N+2)$ control volumes, of which the middle N (in light-gray) are in the flotation section. The dark-gray colored control volume corresponds to the top (outlet) section, whereas the blue colored control volume corresponds to the bottom (outlet) section. All the control volumes have the same volumes and we assume that the water outflow from the initial swirl

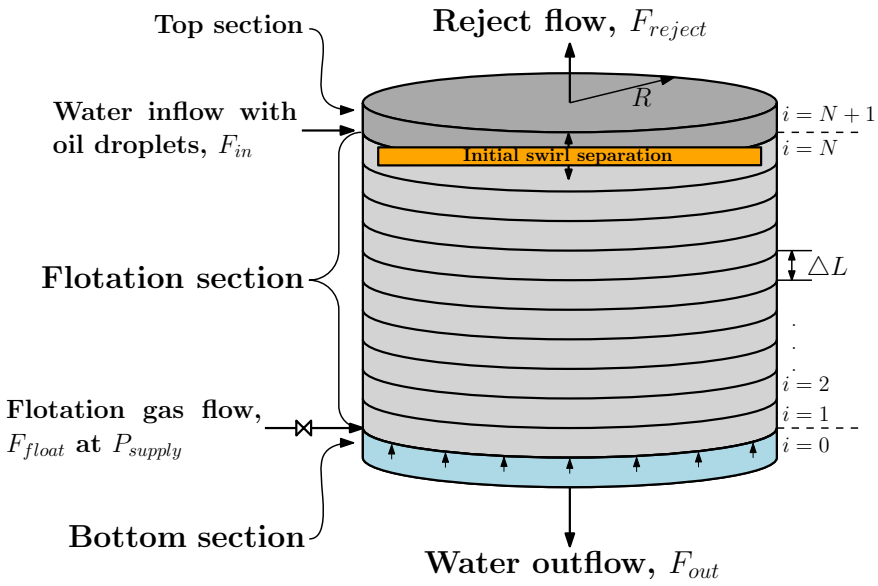

Figure 8: Control volumes. The top section, the bottom section and the flotation section are indicated with the location of introduction of water inflow, reject flow, water outflow and flotation gas inflow. The indices for the control volumes are also shown.

separator enters the flotation section right below the top section, see Figure 8.

First we address the light-gray colored flotation section control volumes and thereafter the blue colored (bottom section) and dark-gray colored (top section).

Flotation section

The control volumes in flotation section are indexed from $i = 1$ to N. We treat the balances on the control volumes differently, depending on if the control volume is at the boundary or in the interior.

Inner control volumes: $i = 2$ to $N - 1$, the balance equation for free bubbles is:

$$\overbrace{\frac{d}{dt}\left(n_{fb}(i)\triangle V\right)}^{Accumulation\ rate} = \overbrace{n_{fb}(i-1)v_{fb}\pi R^2}^{Inflow\ rate} - \overbrace{n_{fb}(i)v_{fb}\pi R^2}^{Outflow\ rate} - \overbrace{L_R\triangle V}^{Consumption\ rate} . \tag{6}$$

After rearrangement, we obtain

$$\frac{dn_{fb}(i)}{dt} = v_{fb}\frac{n_{fb}(i-1) - n_{fb}(i)}{\triangle L} - k\left(\frac{d_d}{d_b}\right)^2 n_{fb}(i)n_d(i). \tag{7}$$

Similar expressions for n_d and n_{lb} results in the following equations

$$\frac{dn_d(i)}{dt} = v_d \frac{n_d(i+1) - n_d(i)}{\triangle L} - k \left(\frac{d_d}{d_b}\right)^2 n_{fb}(i) n_d(i). \tag{8}$$

$$\frac{dn_{lb}(i)}{dt} = v_{lb} \frac{n_{lb}(i-1) - n_{lb}(i)}{\triangle L} + k \left(\frac{d_d}{d_b}\right)^2 n_{fb}(i) n_d(i). \tag{9}$$

The velocity v_{fb} is the absolute velocity of free bubble in the upward direction. The velocity v_d is the absolute velocity of oil droplet in the downward direction. The velocity v_{lb} is the absolute velocity of loaded bubble in the upward direction. A diagrammatic representation of the velocities for the three entities is shown in Figure 9.

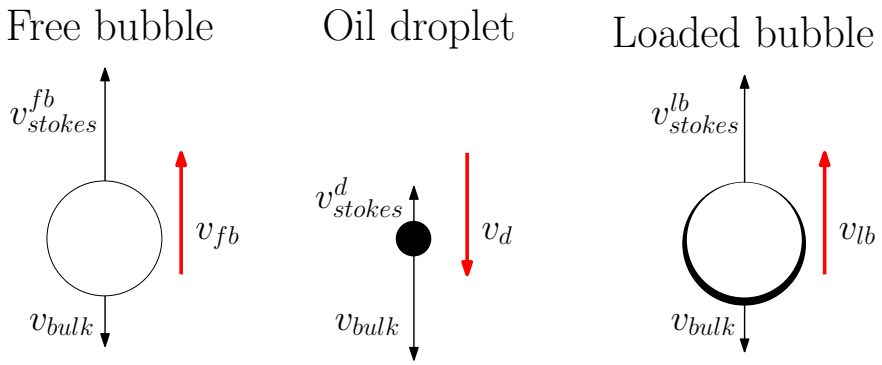

Figure 9: Schematic of velocities. The red arrows indicate the net effect, which is the superposition of the effects indicated by black arrows.

The velocities used in the equations above are derived using Stokes' law.

$$v_{fb} = \overbrace{\frac{(\rho_w - \rho_g)\, g d_b^2}{18\mu_w}}^{v^{fb}_{stokes}} - v_{bulk} \tag{10}$$

$$v_d = v_{bulk} - \overbrace{\frac{(\rho_w - \rho_o)\, g d_d^2}{18\mu_w}}^{v^{d}_{stokes}} \tag{11}$$

$$v_{lb} = \frac{\overbrace{\left(\left(\rho_w - \rho_g\right) V_{fb} + \left(\rho_w - \rho_o\right) V_d\right) g}^{v^{lb}_{stokes}}}{3\pi\mu_w (d_b^3 + d_d^3)^{1/3}} - v_{bulk} \tag{12}$$

$$v_{bulk} = \frac{F_{out}}{(\pi R^2)\,\alpha_l} \tag{13}$$

Here, v_{bulk} represents continuum velocity in the downward direction. F_{out} is volumetric outflow rate of the processed water from the bottom of the separator. α_l is the liquid hold-up inside the separator. The gas density ρ_g is computed using ideal gas law as

$$\rho_g = \frac{PM_g}{R_g T}, \tag{14}$$

where P, M_g, R_g and T are separator pressure, molecular weight of gas, universal gas constant and temperature, respectively.

Control volumes on the boundary in flotation section

For control volume $i = 1$, situated right above the flotation gas inlet, the equations are different from the equations presented for the inner control volumes earlier because of the boundary conditions arising from the inflow of flotation gas and that there is no source term for the loaded bubbles at this control volume. For the free bubbles, the mass balance yields

$$\frac{dn_{fb}(1)}{dt} = \frac{1}{\triangle L}\left(\frac{F_{float}\,(P_{supply}/P)}{V_{fb}\,(\pi R^2)} - v_{fb} n_{fb}(1)\right) - k\left(\frac{d_d}{d_b}\right)^2 n_{fb}(1) n_d(1). \tag{15}$$

Similarly, for n_d and n_{lb} we obtain

$$\frac{dn_d(1)}{dt} = v_d \frac{n_d(2) - n_d(1)}{\triangle L} - k\left(\frac{d_d}{d_b}\right)^2 n_{fb}(1) n_d(1) \tag{16}$$

and

$$\frac{dn_{lb}(1)}{dt} = -v_{lb}\frac{n_{lb}(1)}{\triangle L} + k\left(\frac{d_d}{d_b}\right)^2 n_{fb}(1) n_d(1). \tag{17}$$

Here, F_{float} is flotation gas flow rate supplied at pressure P_{supply}, and V_{fb} is the volume of a free bubble at the separator pressure.

For control volume $i = \mathrm{N}$, below the water feed, the following equations hold. They are different from the inner control volumes because of the boundary conditions arising from the feed of water containing dispersed oil.

$$\frac{dn_{fb}(N)}{dt} = \frac{v_{fb}}{\triangle L}\left(n_{fb}(N-1) - n_{fb}(N)\right) - k\left(\frac{d_d}{d_b}\right)^2 n_{fb}(N)n_d(N) \tag{18}$$

Similar expressions for n_d and n_{lb} result

$$\frac{dn_d(N)}{dt} = \frac{1}{\triangle L}\left(\frac{F_{split}^{down}\epsilon_{in}^{fs}}{V_d\,(\pi R^2)} - v_d n_d(N)\right) - k\left(\frac{d_d}{d_b}\right)^2 n_{fb}(N)n_d(N), \tag{19}$$

where, V_d is the volume of an oil droplet and F_{split}^{down} is obtained using a mass balance on water as

$$F_{split}^{down} = \frac{F_{in}(1-\epsilon_{in})}{(1-\epsilon_{in}^{fs})}, \tag{20}$$

and

$$\frac{dn_{lb}(N)}{dt} = v_{lb}\frac{n_{lb}(N-1) - n_{lb}(N)}{\triangle L} + k\left(\frac{d_d}{d_b}\right)^2 n_{fb}(N)n_d(N). \tag{21}$$

Bottom section

We assume that no free bubble and no loaded bubble manage to reach this section, see Assumption 12. Hence, we do not need to account for their number densities in the bottom section. We only need an equation for the number density of droplets.

$$\frac{dn_d^{bot}}{dt} = \frac{1}{\triangle L}\left(v_d n_d(1) - \frac{F_{out}}{\pi R^2}n_d^{bot}\right). \tag{22}$$

The oil in water at water outlet is computed in *ppm* terms by

$$ppm_{out} = n_d^{bot}V_d \cdot 10^6 \tag{23}$$

Before we present the balance equations for the top section, we need to present the balance for the gas hold-up.

Gas balance

Since there is no chemical reaction, the mass balance of gas is expressed in terms of a molar balance, and the total number of moles of gas in the CFU w_{gas} follows the conservation law

$$\frac{dw_{gas}}{dt} = \dot{w}_{gas,in} - \dot{w}_{gas,out}. \tag{24}$$

Here, $\dot{w}_{gas,in}$ is the molar flow rate of the flotation gas entering the vessel and $\dot{w}_{gas,out}$ is the molar flow rate of the gas removed from the vessel with the reject flow. Using ideal gas law, we reformulate Eq. 24 to

$$\frac{d}{dt}\left(\frac{PV_g}{R_gT}\right) = \left(\frac{P_{supply}F_{float}}{R_gT}\right) - \left(\frac{PF^{gas}_{reject}}{R_gT}\right). \tag{25}$$

Here, P denotes the CFU pressure, F^{gas}_{reject} the gas flow rate in the reject stream and V_g the gas volume inside the separator. Multiplying by R_gT and expanding the left hand side yields

$$V_g\frac{dP}{dt} + P\frac{dV_g}{dt} = \left(P_{supply}F_{float} - PF^{gas}_{reject}\right). \tag{26}$$

Since total CFU volume is fixed, we have $V = V_g + V_l$, where V_l is liquid volume in CFU, differentiating which, we get

$$\frac{dV_g}{dt} = -\frac{dV_l}{dt}. \tag{27}$$

Using Eq. 27, Eq. 26 is further expressed as

$$V_g\frac{dP}{dt} = P\frac{dV_l}{dt} + \left(P_{supply}F_{float} - PF^{gas}_{reject}\right). \tag{28}$$

Using

$$V_g = V - V_l, \tag{29}$$

we can write the pressure equation as

$$\frac{dP}{dt} = \frac{P\left(dV_l/dt\right) + \left(P_{supply}F_{float} - PF_{reject}^{gas}\right)}{V - V_l}. \tag{30}$$

The term $\frac{dV_l}{dt}$ can be obtained from the balance on liquid volume V_l as below taking Assumption 1 (incompressibility of liquids) into account

$$\frac{dV_l}{dt} = F_{in} - F_{out} - \left(F_{reject} - F_{reject}^{gas}\right). \tag{31}$$

The equation can be reformulated in terms of the liquid hold-up $\alpha_l = \left(\frac{V_l}{V}\right)$ as

$$\frac{d\alpha_l}{dt} = \frac{F_{in} - F_{out} - \left(F_{reject} - F_{reject}^{gas}\right)}{V}, \tag{32}$$

where F_{reject}^{gas} can be computed by the equation

$$F_{reject}^{gas} = \alpha_{gas}^{top} F_{reject}. \tag{33}$$

The equation for the hold up of gas in the top section of the CFU α_{gas}^{top} can be found below.

Top section

Based on our assumptions, free bubbles, loaded bubbles and oil droplets separated through initial swirl separation manage to reach this section. The equation for gas hold up in top section α_{gas}^{top} is

$$\frac{d\alpha_{gas}^{top}}{dt} = \frac{1}{\triangle L}\left(V_{fb}(v_{fb}n_{fb}(N) + v_{lb}n_{lb}(N)) - \frac{\alpha_{gas}^{top}F_{reject}}{\pi R^2}\right), \tag{34}$$

and that for oil hold up in top section α_{oil}^{top} is

$$\frac{d\alpha_{oil}^{top}}{dt} = \frac{1}{\triangle L}\left(V_d v_{lb} n_{lb}(N) + \frac{F_{split}^{oil} - F_{reject}^{oil}}{\pi R^2}\right), \tag{35}$$

where, the oil separated at the initial separation that enters the top section directly is

$$F_{split}^{oil} = F_{in}\epsilon_{in} - F_{split}^{down}\epsilon_{in}^{fs} \tag{36}$$

The amount of oil removed through the reject flow F_{reject} is

$$F_{reject}^{oil} = \alpha_{oil}^{top} F_{reject}. \tag{37}$$

Bubble injection model

The flotation gas is supplied at pressure P_{supply}, see Figure 5. When it enters the separator, which has a lower pressure, the volumetric flow rate at CFU pressure P becomes $F_{float}\,(P_{supply}/P)$. The bubbles generated are considered to be of uniform size d_b.

To obtain the flow of number of free bubbles entering between the bottom section and the flotation section, the adjusted flow is then divided by the volume of each bubble V_{fb}. This yields

$$\dot{n}_{fb}^{feed} = \frac{F_{float}\,(P_{supply}/P)}{V_{fb}}. \tag{38}$$

Model summary

In summary, the model consists of the following dynamic states for the case demonstrated by $N = 10$:

- $n_{fb}(i)$, $n_{lb}(i)$ and $n_d(i)$ for all the control volumes indexed $i = 1$ to N, results in $3N$ states.
- n_d^{bot}, α_{gas}^{top} and α_{oil}^{top}.

- Liquid hold-up (α_l) and separator pressure (P)

These result in a total of $(3N + 5)$ differential equations.

Case study

Model parameters

Table 1: Model parameters

Parameter	**Value**
CFU volume, V $[m^3]$	3.2
CFU diameter, $2R$ $[m]$	1.26
CFU height, L $[m]$	2.56
Density of water, ρ_w $[kg/m^3]$	1000
Density of oil, ρ_o $[kg/m^3]$	900
Molecular weight of flotation gas, M_g $[g/mol]$	16
CFU temperature, T $[K]$	300
Universal gas constant, R_g $[J/molK]$	8.314
Bubble diameter at pressure P, d_b $[\mu m]$	200
Gas supply pressure, P_{supply} $[bar]$	2
Droplet diameter, d_d $[\mu m]$	25
Viscosity of water, μ_w $[Pas]$	8.9×10^{-4}
Nominal inlet flow rate, F_{in} $[m^3/h]$	70
Expected range of inlet flow rate, F_{in} $[m^3/h]$	$65 - 80$
Nominal inlet oil in water, ϵ_{in} $[ppm]$	150
Expected range of inlet oil in water, ϵ_{in} $[ppm]$	$125 - 175$
Tuning parameter in loading rate, k $[m^3/s]$	4×10^{-11}
Swirl split pre-factor, A $[-]$	0.4082
Optimum swirl intensity, B $[-]$	0.7
Optimum swirl split, C $[-]$	0.8
Swirl intensity pre-factor, D $[-]$	0.01
Number of discretizations in flotation section, N $[-]$	10

For our case study, we consider a CFU with the parameters given in Table 1. We consider a discretization with $N = 10$. This gives a reasonable trade-off between model size and the ability to demonstrate how the concentration profiles in the CFU behave. The tuning parameter k used in loading rate is considered constant. In operation, the adjustable inputs

are the flotation gas feed rate F_{float}, the reject flow rate F_{reject}, and the water outflow F_{out}. The oily water feed flow rate F_{in} is assumed to be given from an upstream process. We assume that the CFU can be monitored using the measurement vector $y = [P, \alpha_l, ppm_{out}, \alpha_{oil}^{top}, \alpha_{gas}^{top}]^T$. An estimate of α_l can be calculated using differential pressure measurement $\triangle P = (P_{bottom} - P)$ between top and bottom of the separator and assuming that the gas density is negligible in comparison to that of the liquid. Alternatively, the CFU could be weighed to estimate the liquid content. We assume a measurement delay of 1 second, 2 seconds and 30 seconds for the measurements of pressure P, liquid hold-up α_l and water quality ppm_{out}, respectively.

Dynamic model analysis (only stabilizing loop closed)

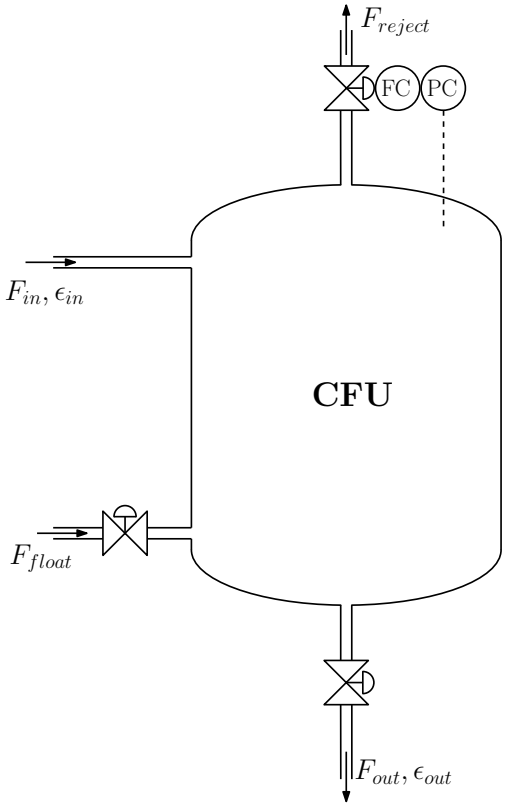

Figure 10: Control loop for CFU with only stabilizing pressure loop closed.

We analyze the dynamic performance of the model with only one stabilizing control loop closed as shown in Figure 10. We close the stabilizing pressure loop in order to control the gas inventory in the separator. The results for operation with the pressure control loop

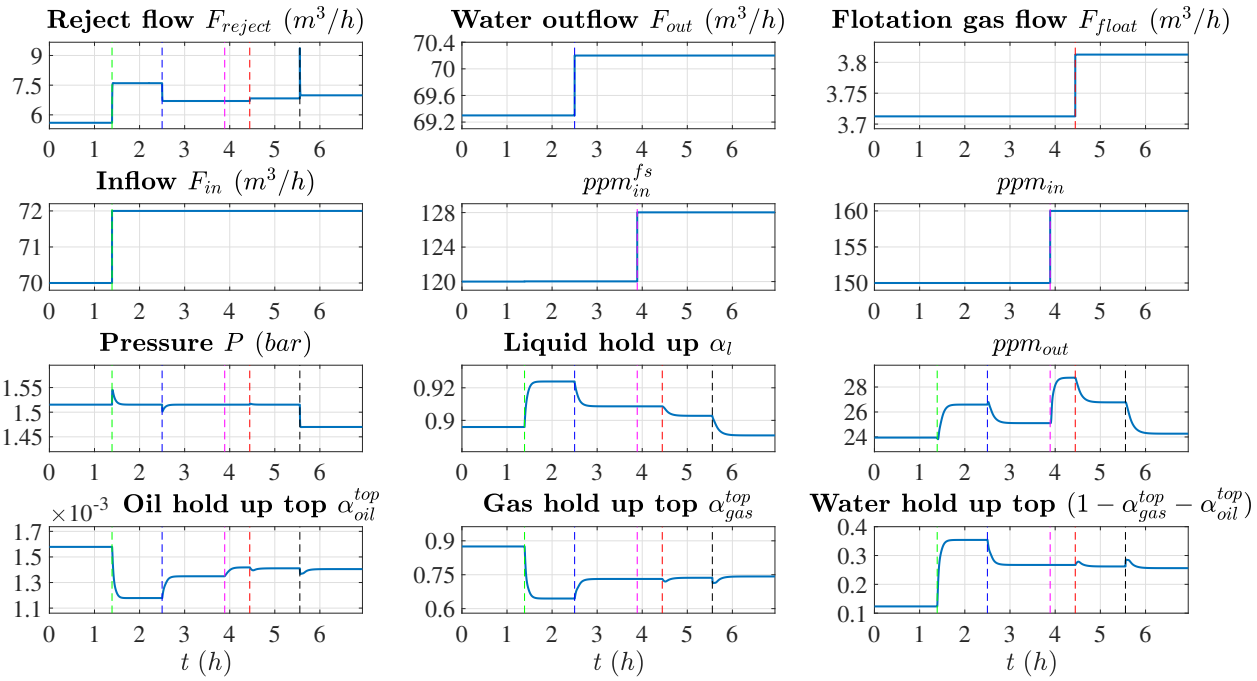

Figure 11: Simulation responses of the CFU model with only a stabilizing pressure control loop closed. The first row of plots are manipulated variables, the second row of plots are disturbance variables, the third row plots are controlled variables and the fourth row of plots are other variables.

closed are in Figure 11, where, we present the effect of the disturbances (F_{in}, ppm_{in}) and the other control inputs (F_{float}, F_{out}) on the outputs. A discussion of the responses is given below.

- **When inflow is raised at 1.39 h**: The liquid hold up increases and settles at a new higher steady state, whereas some additional water escapes through the reject stream. To maintain the pressure, which spikes up because the liquid hold up rises leaving less space for the gas, the reject flow increases due to the pressure control loop. Since more of the water escapes the reject stream, the hold up of oil and gas reduces and that of water increases in the reject stream. ppm_{out} increases because the residence time for separation is reduced leading to worse separation performance.

- **When water outflow is raised at 2.5 h**: The liquid hold up reduces and settles at a new lower steady state, whereas less water escapes through the reject stream.

To maintain the pressure, which spikes downwards because the liquid hold up reduces leaving more space for the gas, the reject flow reduces automatically. Since less of the water escapes the reject stream, the hold up of oil and gas increases and that of water reduces in the reject stream. Since the bulk velocity v_{bulk} rises due to a higher water outflow and a lower liquid hold up, velocities of bubbles v_{fb} and v_{lb} drop. This leads to a higher gas hold up in the system and a higher residence time for bubbles to attach to droplets, which results in an improved separation. Hence, ppm_{out} reduces.

- **When ppm_{in} is raised at 3.89 h**: The oil concentration ppm_{in}^{fs} that enters the flotation section rises. The ppm_{out} goes up because no additional flotation gas is injected to counteract the additional separation load. Due to additional oil in the system, more of the oil escapes the reject stream causing the oil hold up at the top to increase.

- **When flotation gas flow rate is raised at 4.44 h**: The ppm_{out} goes down because additional flotation gas improves the separation performance. Due to additional gas in the system, the pressure spikes, but since the pressure is regulated, the reject flow rate increases to take the additional gas out of the system. The additional gas in the system also causes the liquid hold up to drop and the gas hold up at the top to rise marginally, thereby reducing the oil hold up and water hold up at the top somewhat.

- **When pressure set point is reduced at 5.56 h**: The reject flow rises because lower pressure implies higher gas volume inflow at the separator pressure and reject flow is the only stream that takes gas out of the system. Because of the reduced pressure, the gas occupies more volume, which causes the liquid hold up to drop and the gas hold up at the top to rise. At a lower pressure, the volumetric gas inflow at separator pressure into the bottom of the CFU will be higher for the same gas mass inflow, which means more bubbles at the bottom, leading to higher number of droplet-bubble collisions. This directly increases collision efficiency and thereby, improves the

separation performance. Hence, ppm_{out} reduces as gas is used more effectively at a lower pressure.

Quantitatively, the effects of the inputs and disturbances can be approximated by the gains

$$G^y = \frac{\triangle y}{\triangle u} = \begin{bmatrix} 0 & 0 \\ -0.0581 & -0.0170 \\ -19.8 & -1.6501 \\ 7.05 \times 10^{-5} & 1.89 \times 10^{-4} \\ 0.052 & 0.0962 \end{bmatrix}, \text{and} \tag{39}$$

$$G^d = \frac{\triangle y}{\triangle d} = \begin{bmatrix} 0 & 0 \\ 0.014 & -2.93 \times 10^{-7} \\ 1.320 & 0.36 \\ -2 \times 10^{-4} & 6.88 \times 10^{-6} \\ -0.1151 & -2.93 \times 10^{-7} \end{bmatrix}, \tag{40}$$

where, we recall that $y = [P, \alpha_l, ppm_{out}, \alpha_{oil}^{top}, \alpha_{gas}^{top}]^T$, $u = [F_{float}, F_{out}]^T$ and $d = [F_{in}, ppm_{in}]^T$.

Optimal operation

Control structure design

To design the control structure, we follow loosely the top-down plant-wide control design procedure given by Skogestad.[17] We start by defining the operational objectives, that is the cost function and operational constraints. The objective of operation for the CFU is to minimize the flotation gas flow given by

$$J = F_{float}. \tag{41}$$

There are regulatory requirements of keeping the oil in water outlet below 30 ppm. The

CFU pressure P is required to be between $P_{min} = 1.4$ bar and $P_{max} = 2$ bar as in our case study we consider a topside CFU, which should be operated slightly higher than ambient pressure to ensure outflow of water, and below the upper limit given by design pressure. For reliable operation, the liquid hold up α_l is required to be above 0.85 to avoid gas loss from the bottom of the CFU.

The feed rate F_{in} and the feed composition ϵ_{in} are assumed to be given from an upstream process unit. Their nominal values together with their ranges are given in Table 1. The process has three degrees of freedom that can be manipulated to optimize performance. These are the flotation gas flow rate F_{float}, the water outflow rate F_{out} and the pressure set point P^{set}. The resulting optimization problem is as follows:

$$\begin{aligned} \min_{F_{float}, F_{out}, P^{set}} \quad & F_{float} \\ s.t. \quad & \text{model equations} \\ & ppm_{out} \leq 30\ ppm \\ & 1.4\ bar \leq P \leq 2\ bar \\ & 0.85 \leq \alpha_l \leq 1 \\ & n_d(i), n_{fb}(i), n_{lb}(i) \geq 0 \text{ for all control volumes } i \end{aligned} \tag{42}$$

The optimization problem is solved with the disturbances $d = [F_{in}, ppm_{in}]$ being varied in the expected range around their nominal point $[70\ m^3/h, 150\ ppm]$. For solving the optimization problem we used the IPOPT solver in CasADi library (version 3.3.0) for MATLAB.[18] From the optimization solution, we find:

- The ppm_{out} constraint is active for all disturbance values. This is as expected because any purification below 30 ppm incurs extra cost (flotation gas) that is not necessary.

- The constraint on pressure P is active on the lower limit of 1.4 bar. The objective of minimizing the use of flotation gas implies that the flotation gas has to be used most efficiently. Keeping the pressure as low as possible produces most bubbles for a given

gas mass flow rate, and maximizes the separation.

- The lower limit on the liquid hold-up α_l is active at 0.85. The lower the liquid hold-up, the higher the gas hold up, which indicates more effective use of the flotation gas. A higher gas hold-up indicates a higher number density of the bubbles, which raises the loading rate according to Eq. 3.

At the optimum, therefore, all three degrees of freedom are used for controlling the active constraints. However, in practice we will keep a back-off from the constraint values such that even under disturbances and imperfect control we do not violate the constraints. Hence, we choose the constrained set points as

$$P^{set} = 1.47 \tag{43}$$

$$\alpha_l^{set} = 0.9 \tag{44}$$

$$ppm_{out}^{set} = 25 \tag{45}$$

As in the previous section, we choose to use the reject stream F_{reject} to stabilize the pressure P to set-point P^{set}. The remaining degrees of freedom F_{float} and F_{out} must be then used to control the liquid hold-up α_l and the purity of the water ppm_{out} to their optimal constrained values. We suggest the following:

- ppm_{out} is controlled by the flotation gas flow F_{float}. Flotation gas is the primary agent for separation and directly affects the ppm_{out}. This can be seen from the large value of the gain element $-19.8\ ppm/m^3/h$ in Eq. 39.

- The liquid inventory reflected by liquid hold up α_l needs to be controlled using a flow that has the most liquid content. Hence, water outflow F_{out} is a suitable candidate as an input to control α_l, with a gain of $-0.017\ 1/m^3/h$.

Alongside feedback control to control ppm_{out}, α_l and P using F_{float}, F_{out} and F_{reject}, respectively, the control structure should also be robust to changes in disturbances, especially when the measurement of ppm_{out} is affected by a delay. A possible solution is to implement a ratio controller that controls the ratio F_{float}/F_{in} to a set point $(F_{float}/F_{in})^{sp}$ that is given by the feedback controller for ppm_{out}. Note that the pressure controller, the concentration controller and the hold-up controller are giving the set-points to flow controllers in cascade. See Figure 12 for the entire proposed control structure.

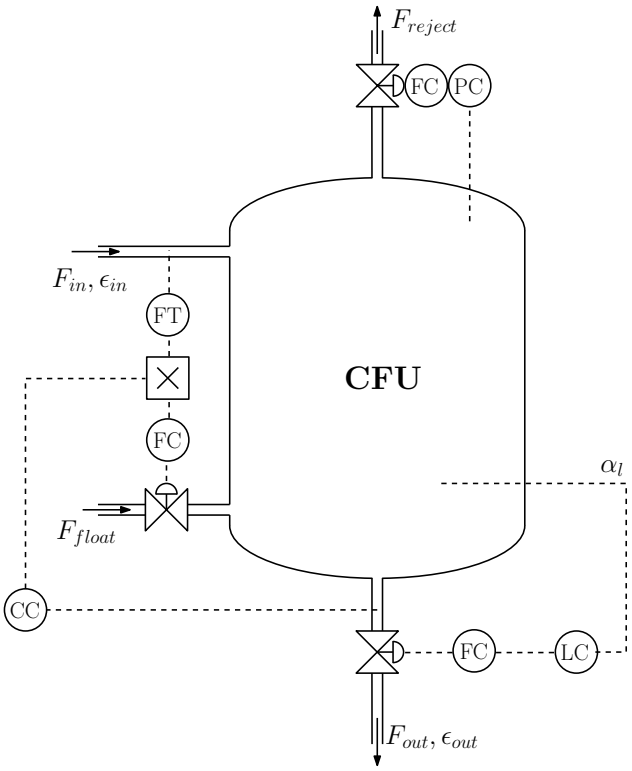

Figure 12: Control loops for CFU with ratio control for water quality.

Steady state operation

From the steady state optimization results, we obtained the set points for the constrained variables $(P, \alpha_l, ppm_{out}) = (1.47, 0.9, 25)$; the disturbances d are $[F_{in}, \epsilon_{in}] = [70\, m^3/h, 150\, ppm]$. The optimal number densities are shown in Figure 13. The flotation gas enters the control volume $i = 1$ from the bottom and flows upwards. Hence, n_{fb} and n_{lb} are zero in the bottom

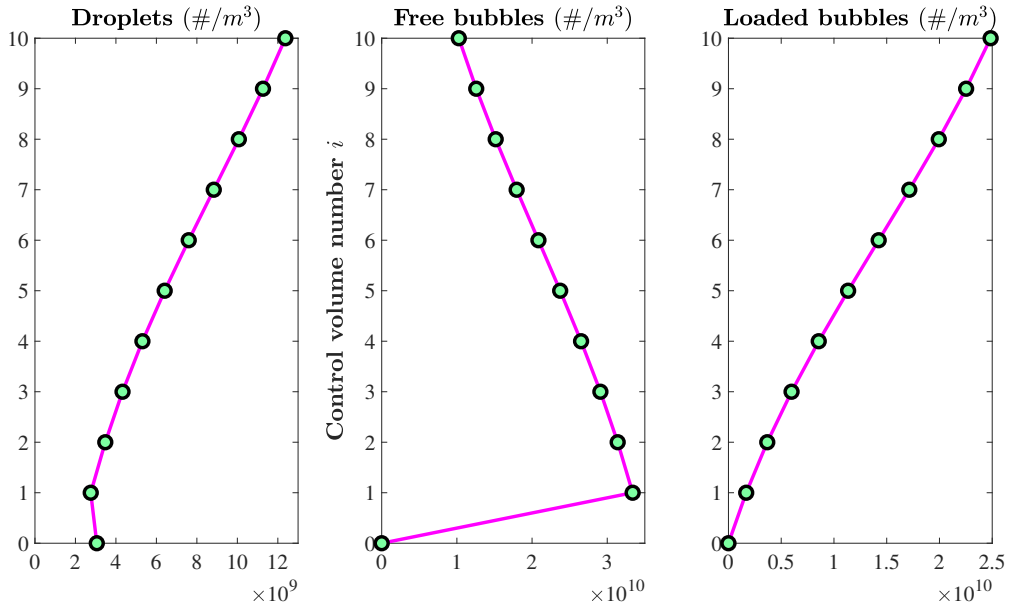

Figure 13: Optimal steady state result describing the number densities of free bubbles, oil droplets and loaded bubbles from the bottom section ($i = 0$) to the section $i = 10$ of CFU.

Table 2: Controller tunings

Control loop	K_c	τ_I [s]
$F_{reject} \rightarrow P$	-55.75	200
$F_{out} \rightarrow \alpha_l$	-318.19	204
$(F_{float}/F_{in})^{sp} \rightarrow ppm_{out}$	-0.0036	316

section $i = 0$ because bubbles cannot move downwards. It can be noticed that from bottom to top, the number density of free bubbles reduces as many of them are converted into loaded bubbles, which is also reflected in an increase in the number density of loaded bubbles from bottom to top. The number density of droplets reduce from top to bottom because some of the droplets get floated by bubbles and travel upwards.

Closed loop dynamic simulation results

For the dynamic simulations, the controller parameters were obtained using the SIMC tuning rules by Skogestad [19] and are given in Table 2 for PI controllers of the form $K_c\left(1 + \frac{1}{\tau_I s}\right)$. As mentioned previously, the optimal set points with back-off compensation are $(P, \alpha_l, ppm_{out}) =$

$(1.47, 0.9, 25)$. To demonstrate our model, starting from suboptimal operation we step the set points one by one to their optimal values. For each of these set point changes, we notice a drop in the consumption of flotation gas. The results from the operation of the CFU are shown in Figure 14 and are discussed below:

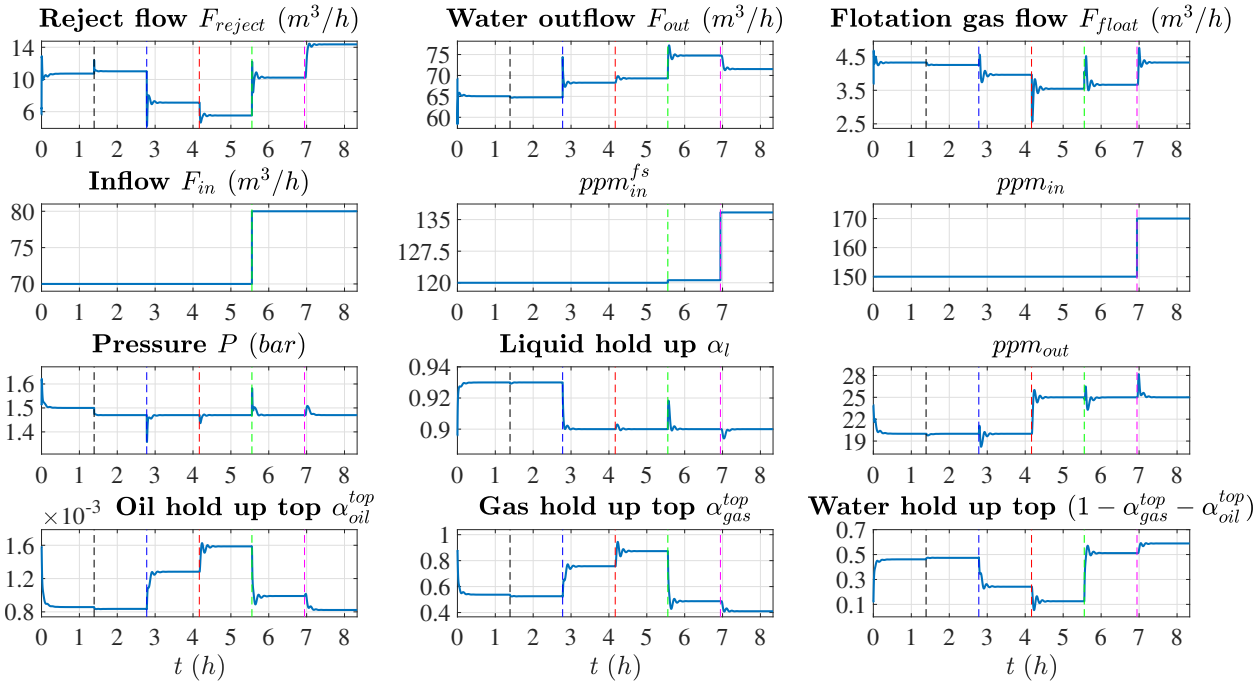

Figure 14: Operation of CFU with active constraint control. The first row of plots are manipulated variables, the second row of plots are disturbance variables, the third row plots are controlled variables and the fourth row of plots are other variables. The operation starts at $t = 0$ with a sub-optimal operating point. The set-points for the controlled variables are changed to bring the system to optimal operation and the cost function - flotation gas flow - shows the benefits. The results also show the closed loop responses on the controlled variables and other important variables to changes in disturbance variables.

- **When pressure set point is reduced at 1.39 h**: The flotation gas is used more effectively as the volume of the flotation gas swells up at a reduced separator pressure according to Eq. 38. A reduced pressure results in more volumetric gas flow rate through the separator (for a given mass flow). As the bubble producing device produces bubbles with a fixed diameter, the increased flow rate will result in a higher free bubble number density and a better separation. The reject outflow is raised to purge the excess volume of the gas phase. As the reject flow carries additional water, the water outflow

reduces in order to maintain the same liquid hold up in the separator. The additional water in the reject causes the oil and gas hold ups to reduce at the top.

- **When liquid hold up set point is reduced at 2.78 h**: The water outflow spikes up and settles at a higher value. A higher water outflow causes less water to exit the reject flow. A reduced liquid hold up provides excess space for the gas, leading to an intermittent drop in pressure, while a higher gas hold up in the system leads to an effective usage of flotation gas. Therefore, a reduced flotation gas inflow is necessary to meet the ppm_{out} set point. A higher gas hold up is also present in the top section, causing oil and water hold ups at the top to drop. The reduction in flotation gas inflow causes an overall reduction in reject flow.

- **When ppm_{out} set point is raised at 4.17 h**: The flotation gas inflow reduces as the cleaning load is reduced. A reduced gas inflow causes pressure to drop transiently until it is recovered by the pressure controller. A higher ppm_{out} set point also causes a reduction in loss of water in the reject stream. Hence, at the top the hold up of water drops, while that of oil and gas rise. Overall, the reject flow reduces due to reduced water and gas flows in the reject stream.

- **Rejection of disturbance - inflow raised at 5.56 h**: The pressure spikes up causing the reject flow to be raised to maintain the pressure set point. A higher pressure in the transients make the gas occupy less volume, which results in liquid hold up rising transiently. The water outflow also rises to keep the liquid hold up at the set point as well as to compensate for the additional inflow. The oil concentration ppm_{in}^{fs} rises because at a higher flow, the swirl intensity increases causing an increase in the swirl split. In addition, because of a reduced residence time in CFU, keeping the ppm_{out} at the set point requires additional flotation gas. The ratio controller for ppm_{out} causes a quick rise in flotation gas proportional to the step in inflow, which results in a shorter spike in ppm_{out}. Because of an additional inflow, the water content in the

reject increases, and at the same time the gas hold up and the oil hold up in the top fall.

- **Rejection of disturbance - ppm_{in} raised at 6.94 h**: The oil concentration ppm_{in}^{fs} rises. The ppm_{out} spikes up causing more flotation gas to be used due to automatic regulation of ppm_{out}. This also causes the pressure to spike up transiently, which is counteracted by an increase in reject flow. An increased reject flow causes a higher amount of water to escape through the reject stream. This leads to a higher water hold up at top causing the gas hold up and the oil hold up at the top to fall. Since the overall liquid hold up is regulated at a fixed set point, water outflow drops.

Discussion and future work

Several simplifying assumptions have been considered in this paper to develop a simplified CFU model. These assumptions are discussed below.

The bubble injection model assumes that the bubbles produced are of a specific uniform size, which depends on the design of the bubble producing device. Depending on the actual design, the bubble size will change with the pressure in the CFU, but we chose not to model this effect because we do not have any information about the details of such devices. Also, there will be a pressure gradient in the separator with higher pressure towards the bottom of the separator, which will cause the bubbles to slightly grow in size as they rise from the bottom of the separator. A larger bubble size may lead to a poorer separation efficiency as given by Eq. 4. The pressure difference between top and bottom of the separator is relatively small. Therefore, we have chosen not to include this effect in the model as its effect is relatively small in comparison to the effect that other modeling assumptions have.

We introduced a simple model - Eq. 1 - to describe the swirl effect in the CFU. For the parameters we have chosen, the swirl split has a minimum value of 0.8 at swirl intensity 0.7. These values can be considered tuning parameters, which can be adjusted to match

operational data. Alternatively, if more information about a particular design were available, one could include a more detailed model of the swirl into the CFU model.

In the modeled CFU design, the inlet swirl separator is designed to promote separation and coalescence, such that the droplets exceeding a certain size will be separated and removed, while smaller droplets coalesce to form larger droplets that enter the flotation section. These two effects contribute to a narrow oil droplet size distribution that enters the flotation section. Based on this phenomenon, we chose to develop a model that assumes a single representative droplet size for all droplets. This representative droplet size need not necessarily be the mean of the true droplet size distribution, as it may be adjusted to match the model outlet purities to real data. This kind of approach is not uncommon for the design of systems with dispersed phases. Examples of such simplifications include the use of the Sauter mean diameter,[20] or the use of mass median diameters, such as d_{50}.[21]

A distribution in oil droplet sizes as well as in bubble sizes could, however, be included in the model we have developed. For each additional droplet class, two additional equations for number densities - one for droplet and the other for loaded bubble - need to be considered for each control volume in the bottom section and the flotation section, whereas for each additional bubble class, two additional equations for number densities - one for free bubble and the other for loaded bubble - need to be considered for each control volume in flotation section. In the top section, the gas inflow from each free and loaded bubble class needs to be considered and oil inflow from each loaded bubble class needs to be considered. If distributions in both oil droplet and gas bubble sizes are considered, then the number of equations for number density of loaded bubbles will increase corresponding to each possible combination of individual droplet and individual bubble class. However, this would add significantly to the model complexity, and for the purposes of optimal operation and control (especially for finding active constraints), this is usually not necessary.

As mentioned above, the collision efficiency tuning parameter k can be used to describe the swirling turbulence effect that is not captured in the initial swirl separator model. It could

also be adapted to account for un-modeled phenomena such as improved separation due to coalescence in the flotation section. By stacking several models of the type we have described, one can also describe more sophisticated designs, e.g. the ones by *Schlumberger*,[11,12] and by *Siemens Water Technologies Corporation*,[13] where the flotation gas and the produced water enter the CFU together from the same inlet and the produced water goes through multiple stages of separation.

In this work, we did not have the possibility to validate the model against real data or a validated high-fidelity model. However, if operational data for a particular CFU design becomes available in future, this model can be used as a starting point and adapted to make it more representative of the real process. Also, it can be used in a design of experiments framework to determine good experiments that can be used to either validate the model, or decide where it needs to be improved.

Conclusion

In this paper, a control oriented dynamic model for a compact flotation unit has been presented. To the authors' knowledge this is the first control-oriented model of a CFU that is available in the literature. The main motivation of the work is to understand the CFU flotation process from the point of view of control in order to develop a effective control scheme. An analysis of the model and its behavior under manual and automatic control has been presented. The model has been qualitatively verified for expected behavior. It has been shown that a simple PI based decentralized control structure can function well despite multi-variable couplings between the inputs and the outputs. Further, the model has been used to optimize the operating conditions. The optimal solution is found to lie at the boundary of the feasible region and has been implemented as active constraint control. Simulations have been performed starting at a suboptimal point and moving towards optimal operation. The changes in the disturbances were also handled effectively by the control structure, which

ensured that the set points are maintained.

Acknowledgement

The authors acknowledge funding from the SUBPRO (Subsea production and processing) center for research-based innovation and the Norwegian Research Council.

References

(1) Fakhru'l-Razi, A.; Pendashteh, A.; Abdullah, L. C.; Biak, D. R. A.; Madaeni, S. S.; Abidin, Z. Z. Review of technologies for oil and gas produced water treatment. *Journal of hazardous materials* **2009**, *170*, 530–551.

(2) Discharges, OSPAR Convention. 2001; `https://www.ospar.org/work-areas/oic/discharges`.

(3) Pavelic, P.; Vanderzalm, J.; Dillon, P.; Herczeg, A.; Barry, K.; Levett, K.; Mimoso, J.; Magarey, P. Assessment of the potential for well clogging associated with salt water interception and deep injection at Chowilla, SA. *Final Report to Department of Water, Land, Biodiversity and Conservation* **2007**, 13–27.

(4) Arvoh, B. K.; Asdahl, S.; Rabe, K.; Ergon, R.; Halstensen, M. Online estimation of reject gas and liquid flow rates in compact flotation units for produced water treatment. *Flow Measurement and Instrumentation* **2012**, *24*, 63–70.

(5) Asdahl, S.; Rabe, K. Real-time automatic operation and optimization of produced-water treatment. SPE Middle East Intelligent Energy Conference and Exhibition. 2013.

(6) Arvoh, B. K.; Asdahl, S.; Rabe, K.; Halstensen, M. Online estimation of reject gas flow rates in compact flotation units for produced water treatment: A feasibility study. *Chemometrics and Intelligent Laboratory Systems* **2012**, *114*, 87–98.

(7) Frankiewicz, T.; Lee, C.-M.; Juniel, K. Compact induced gas flotation as an effective water treatment technology on deep water platforms. Offshore Technology Conference. 2005.

(8) Rawlins, C. H.; Ly, C. Mechanisms for Flotation of Fine Oil Droplets. *Separation Technologies for Minerals, Coal, and Earth Resources* **2012**, 307.

(9) Moosai, R.; Dawe, R. Oily wastewater cleanup by gas flotation. *West Indian J. Eng* **2002**, *25*, 25–41.

(10) Shannon, D. Developments in Micro-footprint, Multi-stage Flotation. 2016.

(11) Bhatnagar, M.; Sverdrup, C. J. Advances in Compact Flotation Units (CFUs) for Produced Water Treatment. Offshore Technology Conference-Asia. 2014.

(12) Maelum, M.; Rabe, K. Improving oil separation from produced water using new compact flotation unit design. SPE Production and Operations Symposium. 2015.

(13) Hayatdavoudi, A.; Howdeshell, M.; Godeaux, E.; Pednekar, N.; Dhumal, V. Performance analysis of a novel compact flotation unit. *Journal of energy resources technology* **2011**, *133*, 013101.

(14) Eftekhardadkhah, M.; Aanesen, S. V.; Rabe, K.; Øye, G. Oil Removal from Produced Water during Laboratory-and Pilot-Scale Gas Flotation: The Influence of Interfacial Adsorption and Induction Times. *Energy & Fuels* **2015**, *29*, 7734–7740.

(15) Tyvold, P. F. Modeling and optimization of a subsea oil-water separation system. M.Sc. thesis, NTNU, 2015.

(16) Oliveira, R.; Gonzalez, G.; Oliveira, J. Interfacial studies on dissolved gas flotation of oil droplets for water purification. *Colloids and Surfaces A: Physicochemical and Engineering Aspects* **1999**, *154*, 127–135.

(17) Skogestad, S. Control structure design for complete chemical plants. *Computers & Chemical Engineering* **2004**, *28*, 219–234.

(18) Andersson, J. A general-purpose software framework for dynamic optimization. Ph.D. thesis, Arenberg Doctoral School, KU Leuven, Department of Electrical Engineering (ESAT/SCD) and Optimization in Engineering Center, Kasteelpark Arenberg 10, 3001-Heverlee, Belgium, 2013.

(19) Skogestad, S. Simple analytic rules for model reduction and PID controller tuning. *Journal of process control* **2003**, *13*, 291–309.

(20) Kowalczuk, P. B.; Drzymala, J. Physical meaning of the Sauter mean diameter of spherical particulate matter. *Particulate Science and Technology* **2016**, *34*, 645–647.

(21) Neumann, L.; White, E.; Howes, T., et al. What does a mean size mean? Chemeca 2003: Products and Processes for the 21st Century: Proceedings of the 31st Australasian Chemical Engineering Conference. 2003; p 928.

Graphical TOC Entry